


























ARTICLE

Production of high-quality SARS-CoV-2 antigens: Impact of bioprocess and storage on glycosylation, biophysical attributes, and ELISA serologic tests performance

Rute Castro¹  | Lígia S. Nobre¹  | Rute P. Eleutério¹  | Mónica Thomaz^{1,2}  |
 António Pires¹  | Sandra M. Monteiro¹  | Sónia Mendes¹  |
 Ricardo A. Gomes¹  | João J. Clemente¹  | Marcos F. Q. Sousa^{1,2}  |
 Filipe Pinto¹  | Ana C. Silva¹  | Micael C. Freitas^{1,2}  | Ana R. Lemos^{1,2}  |
 Onome Akpogheneta³  | Lindsay Kosack³  | Marie-Louise Bergman³  |
 Nadia Duarte³  | Paula Matoso³  | Júlia Costa²  | Tiago M. Bandejas^{1,2}  |
 Patricia Gomes-Alves^{1,2}  | Carlos P. Gonçalves³  | Jocelyne Demengeot³  |
 Paula M. Alves^{1,2} 

¹iBET, Instituto de Biologia Experimental e Tecnológica, Oeiras, Portugal

²ITQB NOVA, Instituto de Tecnologia Química e Biológica António Xavier, Universidade Nova de Lisboa, Av. da República, Oeiras, Portugal

³IGC, Instituto Gulbenkian de Ciência, Oeiras, Portugal

Correspondence

Paula M. Alves, iBET, Instituto de Biologia Experimental e Tecnológica, Apartado 12, 2780-901, Oeiras, Portugal.
 Email: marques@ibet.pt

Abstract

Serological assays are valuable tools to study SARS-CoV-2 spread and, importantly, to identify individuals that were already infected and would be potentially immune to a virus reinfection. SARS-CoV-2 Spike protein and its receptor binding domain (RBD) are the antigens with higher potential to develop SARS-CoV-2 serological assays. Moreover, structural studies of these antigens are key to understand the molecular basis for Spike interaction with angiotensin converting enzyme 2 receptor, hopefully enabling the development of COVID-19 therapeutics. Thus, it is urgent that significant amounts of this protein became available at the highest quality. In this study, we produced Spike and RBD in two human derived cell hosts: HEK293-E6 and Expi293F™. We evaluated the impact of different and scalable bioprocessing approaches on Spike and RBD production yields and, more importantly, on these antigens' quality attributes. Using negative and positive sera collected from human donors, we show an excellent performance of the produced antigens, assessed in serologic enzyme-linked immunosorbent assay (ELISA) tests, as denoted by the high specificity and sensitivity of the test. We show robust Spike productions with final yields of approx. 2 mg/L of culture that were maintained independently of the production scale or cell culture strategy. To the best of our knowledge, the final yield of 90 mg/L of culture obtained for RBD production, was the highest reported to date. An in-depth characterization of SARS-CoV-2 Spike and RBD proteins was performed, namely the antigen's oligomeric state, glycosylation profiles, and thermal stability during storage. The correlation of these quality attributes with ELISA

This is an open access article under the terms of the Creative Commons Attribution-NonCommercial-NoDerivs License, which permits use and distribution in any medium, provided the original work is properly cited, the use is non-commercial and no modifications or adaptations are made.

© 2021 The Authors. *Biotechnology and Bioengineering* Published by Wiley Periodicals LLC

performance show equivalent reactivity to SARS-CoV-2 positive serum, for all Spike and RBD produced, and for all storage conditions tested. Overall, we provide straightforward protocols to produce high-quality SARS-CoV-2 Spike and RBD antigens, that can be easily adapted to both academic and industrial settings; and integrate, for the first time, studies on the impact of bioprocess with an in-depth characterization of these proteins, correlating antigen's glycosylation and biophysical attributes to performance of COVID-19 serologic tests.

KEYWORDS

bioprocess, COVID-19, ELISA, glycosylation, production and purification, RBD, SARS-CoV-2, serologic assay, Spike, thermal stability during storage

1 | INTRODUCTION

COVID-19 caused by SARS-CoV-2 virus was first detected in the Wuhan region in China, in December 2019 (Zhou et al., 2020). In March 2020, COVID-19 outbreak was declared pandemic by the World Health Organization (WHO) and, by mid-December 2020, the virus was responsible for the infection of more than 75 million people and caused 1.7 million deaths worldwide (WHO, Coronavirus Disease Dashboard).

The development of serological assays to study the human response to SARS-CoV-2 has been reported (Amanat et al., 2020; Okba et al., 2020; Perera et al., 2020; Weiss et al., 2020). It is well known that some infected individuals are asymptomatic. Therefore, a broad application of serological assays will provide clear epidemiological data regarding the SARS-CoV-2 infection, as well as the real mortality rates for COVID-19. Moreover, the identification of individuals that were already infected, and therefore, would possibly be immune to virus reinfection, has important social and economic impact. Serological assays based on SARS-CoV-2 Spike protein and its receptor binding domain (RBD), present good sensitivity and specificity (Amanat et al., 2020; Okba et al., 2020).

SARS-CoV-2 Spike glycoprotein mediates virus entry in the target cells via its binding to the angiotensin converting enzyme 2 (ACE2) receptor. The determination of SARS-CoV-2 Spike protein structure, provided good indications for the development of vaccines and inhibitors (Walls et al., 2020; Wang et al., 2020; Wrapp et al., 2020). Additionally, despite the high structural similarity between Spike proteins from SARS-CoV-2 and SARS-CoV viruses, no antibody cross-reactivity has been detected (Wrapp et al., 2020). Characterization of Spike glycosylation profile as been the subject of several studies, due to its perceived importance on the development of COVID-19 therapies or prophylaxis (Shajahan et al., 2020; Watanabe et al., 2020). Indeed, mapping of SARS-CoV-2 Spike glycosylation using a cryo-EM structure of the protein suggested the shielding of RBD by proximal glycans (Watanabe et al., 2020).

With the ultimate goal of providing high-quality substrates to perform SARS-CoV-2 serological assays, we investigated the production process for Spike and RBD antigens, using two human cell hosts, HEK293-E6 (Durocher et al., 2002) and Expi293F™. Different

cell culturing approaches and production scales were evaluated. The impact of downstream processing (DSP) steps and distinct storage temperature conditions were also assessed. An in-depth characterization of the antigens was performed correlating oligomeric state, glycosylation profile, and thermal stability with the bioprocess set-up and the storage conditions. Finally, the quality of the antigens was assessed in enzyme-linked immunosorbent assay (ELISA) serological tests using human serum control samples.

2 | MATERIALS AND METHODS

2.1 | Recombinant proteins

Plasmid DNA for the expression of SARS-CoV-2 Spike and Spike's RBD was kindly provided by Prof. Florian Krammer (Icahn School of Medicine at Mount Sinai). Soluble Spike protein presents a T4 foldon trimerization domain, a C-terminal hexahistidine tag, two stabilizing mutations and includes the removal of polybasic cleavage site (further details described by Amanat et al., 2020). Soluble RBD includes the signal peptide and C-terminal hexahistidine tag. Transfection grade plasmids were obtained from 2.5 L cultures of *Escherichia coli* DH5 α transformed with Spike or RBD expression vectors, using the Qiagen Giga Prep kit (Qiagen) or equivalent, following the manufacturer instructions.

2.2 | Cell lines, culture conditions, and cell concentration determination

In this study we used two human embryonic kidney derived cell lines: HEK293-E6 cells (Durocher et al., 2002) and Expi293F™ cells (Thermo Fisher Scientific). HEK293-E6 cells were cultured in suspension in FreeStyle™ F17 expression medium, supplemented with 4 mM Glutamax, 0.1% Pluronic F-68 and 25 μ g/ml of Geneticin, in shake flasks at 37°C in a humidified atmosphere of 5% CO₂ in air, and stirring rates of 75 or 90 rpm. Expi293F™ cells were cultivated in Expi293™ Expression Medium, according to the manufacturer instructions. All media and cell culture supplements were from Thermo Fisher Scientific.

Cell concentration and viability was determined by the trypan blue (Gibco) exclusion method using a 0.1% (v/v) solution prepared in Dulbecco's phosphate-buffered saline (Gibco) and counting cells in a Fuchs Rosenthal haemocytometer (Brand) using an inverted microscope (Olympus CK40). Viable cell concentration was also monitored using NucleoCounter® NC-200™ (Chemometec).

2.3 | Spike and RBD production in human cell lines

Exponentially growing HEK293-E6 cells were transiently transfected with 1 mg of plasmid DNA per liter of culture, complexed with polyethylenimine (PEI, Polysciences), in a DNA:PEI ratio of 1:2. Six hours posttransfection, 0.5 mM of valproic acid (Merck KGaA), a histone deacetylase inhibitor, was added to the cultures to improve transient gene expression. Cell concentration and viability were monitored every day and cultures were harvested 3–5 days posttransfection. Three different cell culturing strategies were tested: 2.5 L culture volume in 5 L in shake flasks (Corning), stirred tank bioreactors (STB) of 2 and 5 L working volume (Biostat DCU-3; Sartorius) and wave-mixed bioreactors up to 30 L (Biostat Cultibag RM; Sartorius). In STB, dissolved oxygen (DO) was kept at 40% (of air saturation) by sequentially varying stirring rate and the percentage of oxygen in gas inlet, at a constant aeration rate of 0.01 vvm using ring-sparger. pH was controlled at 7.2 by the addition of CO₂ or NaHCO₃ and temperature was controlled at 37°C using a heating jacket. The wave-mixed bioreactor cultures were performed at rocking angle of 8°, 18 rocks/min, and a continuous supply of air with 5% of CO₂ through the headspace, at a rate of 0.02 vvm. Temperature was maintained at 37°C. Process control and monitoring was carried out using Multi Fermenter Control Software (Sartorius).

For the Expi293F™ cells, shake flask cultures at 1 L scale were used, and transient transfection was performed as described in the manufacturer instructions. Cell concentration and viability were monitored every day and the cultures were harvested at 3 days posttransfection. The bulk from 5 cultures (5 L), *per* Spike or RBD production run, was pooled together and purified as described below.

The impact of decreasing the temperature to 32°C during protein expression and lowering the coding DNA amount to 50% (0.5 µg/ml of culture) was also evaluated at small scale (25 ml shake flasks cultures). For the 32°C experiments, cells were transfected as described above and, 18 h posttransfection, the cultures were moved to an incubator at 32°C. In the 50% DNA experiments, transfection was performed with a total of 1 µg DNA/ml of culture consisting of 0.5 µg of Spike or RBD expression vector and 0.5 µg of empty pTT5™ expression vector per ml of culture. Cell concentration and viability were monitored every day and culture supernatants were analyzed by sodium dodecyl sulfate polyacrylamide gel electrophoresis (SDS-PAGE).

For all the experimental production set-ups glucose, lactate, glutamine, glutamax, glutamate and ammonia were quantified in culture supernatants using Cedex Bio analyzer (Roche).

2.4 | Protein purification and quantification

At Day 3–5 posttransfection, cell culture bulks were clarified by centrifugation at 2000g for 20 min at 4°C, followed by filtration using 0.2 µm filters (Sartopore 2; Sartorius). Tangential flow filtration (TFF) was used to concentrate and dialyse the clarified supernatants to 50 mM sodium phosphate supplemented with 300 mM NaCl and 20 mM imidazole, at pH 7.4 (binding buffer). Membranes of 10 and 30 kDa (Sartorius) were used for RBD and Spike, respectively.

After the TFF step, a chromatographic step was performed in Äkta systems (GE Healthcare) using HisTrap HP columns (GE Healthcare), previously equilibrated with binding buffer. Two washing steps with 35 and 50 mM imidazole were performed, and proteins were eluted with a linear gradient up to 500 mM imidazole. Spike and RBD eluted from the nickel affinity chromatography (AC) were concentrated using vivaflow 200 crossflow device (Sartorius) and subjected to size exclusion chromatography (SEC) using Superdex 200 or Superdex 75 columns (GE Healthcare), respectively, previously equilibrated with phosphate-buffered saline at pH 7.4 (PBS; formulation buffer). The proteins eluted from SEC were concentrated using vivaflow 200 crossflow device or amicon® ultra centrifugal units (Merck KGaA), filtered through polyethersulfone membranes with 0.2 µm, flash frozen in liquid nitrogen and stored at -80°C.

In the STB production runs, to reduce further processing time and product losses, the SEC step was replaced by buffer exchange using vivaflow 200 crossflow devices and performing dialysis with minimal of 10 volumes of formulation buffer.

For purification of RBD produced in Expi293F™ cells, an additional washing step at 68 mM imidazole was included before elution with linear gradient to 500 mM imidazole, to improve protein purity. Additionally, the protein fractions eluted from AC were desalted to formulation buffer, using G25 Sephadex desalting column (GE Healthcare).

Alternatively, wave-mixed bioreactor bulks containing Spike protein were also purified performing the clarification step with high-capacity filters of 1.8 m² filtration area and 0.45 µm/0.2 µm pore size (Sartopore 2 MaxiCaps, Sartorius), and the protein eluted from AC was subjected to concentration and dialysis using vivaflow 200 crossflow device (Sartorius). This way the centrifugation and SEC steps were avoided.

Protein concentration was determined by A_{280nm} combined with the specific extinction coefficients, using MySpec spectrophotometer (VWR). Final purified products were also quantified by Thermo Fisher Scientific Pierce™ BCA Protein Assay Kit and Pierce™ Coomassie Plus (Bradford) Assay reagent.

SDS-PAGE analysis was performed by loading protein samples on 4–12% bis-tris NuPAGE gels (Thermo Fisher Scientific) using 3-(N-morpholino)propanesulfonic acid buffer and standard running conditions. For reducing conditions, 200 mM of dithiothreitol (DTT) was added to loading buffer and protein samples were heated at 100°C for 3 min. Protein bands were revealed by incubation with InstantBlue™ (Expedeon Protein Solutions) and SDS-PAGE destaining was performed in water.

2.5 | Spike and RBD characterization

2.5.1 | High-performance liquid chromatography (HPLC) analysis

Spike and RBD samples were analysed in an HPLC system equipped with Photodiode Array Detector (Waters). Spike samples were injected in XBridge BEH 200 Å SEC 3.5 µm or XBridge BEH 450 Å SEC 3.5 µm HPLC columns (Waters), at 0.86 ml/min, using as mobile phase PBS pH 7.4. RBD samples were injected in XBridge BEH 125 Å SEC 3.5 µm HPLC column (Waters) at 0.86 ml/min using as mobile phase PBS with 0.5 M of arginine at pH 7.4. Twenty micrograms of protein were injected in each HPLC run.

2.5.2 | Differential scanning fluorimetry (DSF)

DSF was performed in MicroAmp™ EnduraPlate™ Optical 96-Well Clear Reaction Plates with Barcode (Applied Biosystems) using a QuantStudio 7 Flex Real-Time PCR System (Applied Biosystems). Protein samples were centrifuged for 15 min before preparation. The final reaction mixture contained 4 µg of either Spike or RBD protein and Protein Thermal Shift™ Dye (1000× stock; Applied Biosystems) diluted 1:250 in PBS pH 7.4. Melting curve data were recorded from 15°C to 90°C with an increment rate of 0.016°C/s. Excitation and emissions filters were applied for Protein Thermal Shift™ Dye (470 and 520 nm, respectively) and for ROX reference dye (580 and 623 nm, respectively). The melting temperatures were obtained by calculating the midpoint of each transition, using the Protein Thermal Shift Software™ version 1.3. All samples were tested in duplicates.

2.5.3 | Nano differential scanning fluorimetry (NanoDSF)

NanoDSF was performed on a Prometheus NT.48 instrument (NanoTemper Technologies GmbH). Protein samples were centrifuged for 15 min before preparation. The final reaction mixture contained 4 µg of either Spike or RBD proteins diluted in PBS pH 7.4. High sensitivity capillaries (NanoTemper Technologies) were filled with 10 µl of sample and placed on the sample holder. A temperature gradient of 1°C/min was applied from 15°C to 95°C and the intrinsic protein fluorescence at 330 and 350 nm was recorded. Data were analysed using either the value of fluorescence at 330 nm (for Spike protein) or the derived ratio 350/330 value (for RBD protein). All samples were tested in duplicates.

2.5.4 | Dynamic light scattering (DLS) analysis

A SpectroLight 610 (Xtal Concepts GmbH) was used to carry out serial DLS measurements. All samples were centrifuged (15–30 min, 4°C, 17200g) in a benchtop centrifuge before measurements and were pipetted (each sample in duplicate, 1 µl per well) onto a 96-well

Vapor Batch Plate (Jena Bioscience GmbH). Before usage, the plates were filled with paraffin oil (Cat N. 18512; Merck) to protect sample solutions from drying out. The laser wavelength was 660 nm at a power of 100 mW. The scattering angle for placement of the detector was fixed at 142°. All tested samples were kept in PBS buffer, therefore, the refractive index (1.34) and viscosity (1.006) of water were used for calculations. All samples were measured at constant 20°C, one scan per drop with 20 measurements of 20 s each.

2.5.5 | Glycosylation pattern analysis by LC-MS, lectin blotting, and glycosidase digestion

Proteins were analyzed by SDS-PAGE and transferred to polyvinylidene fluoride membranes, which were blocked with 3% BSA biotin free (Carl-Roth) in tris buffered saline supplemented with tween 20 (TBST) for 1 h. Then, membranes were incubated with lectins from *Wisteria floribunda* agglutinin (WFA; Vector Laboratories), *Maackia amurensis* lectin (MAL), *Sambucus nigra* agglutinin (SNA), *Aleuria aurantia* lectin (AAL), and *Galanthus nivalis* agglutinin (GNA; Galab Technologies), at 1 µg/ml in TBST for 1 h. Blots were washed with TBST and incubated with 0.1 µg/ml streptavidin-peroxidase (Merck KGaA) for 1 h. Blots were washed, and detection was performed with the Immobilon Western chemiluminescent HRP substrate (Millipore).

Glycoproteins were digested with peptide N-glycosidase F (PNGase F; ProZyme, Agilent), endoglycosidase H (Endo H; Roche) and sialidase from *Arthrobacter urefaciens* (Roche) as previously described (Escrevente et al., 2011; Machado et al., 2011).

The glycosylation profiling of Spike and RBD proteins was further assessed using LC-MS analysis of glycopeptides. Thirty micrograms of protein sample were subjected to trypsin digestion. Briefly, protein sample was denatured with 6 M guanidine hydrochloride, reduced with 10 mM DTT (Merck KGaA) for 15 min at 56°C followed by alkylation with 20 mM iodoacetamide (Merck KGaA) for 30 min in the dark. Excessive iodoacetamide was quenched by further incubation with DTT (10 mM for 10 min in the dark). A step of buffer exchange was performed using Zeba Spin desalting plates (Thermo Fisher Scientific). The resulting sample was digested overnight with trypsin (Proteomics grade from Promega) at 37°C (1:50 protein:trypsin ratio). Trypsin digestion was stopped with the addition of formic acid (1% final concentration).

Glycopeptides were analysed by LC-MS using an X500B-QTOF mass spectrometer (SCIEX) connected to an ExionLC AD UPLC system. LC separation was achieved through reversed-phase chromatography using an XBridge BEH C18, 2.5 µm 2.1 × 150 mm (Waters). Separation was performed at 200 µL/min with 0.1% formic acid in water LC-MS grade as solvent A and 0.1% formic acid in acetonitrile as solvent B, and column temperature was set to 40°C. The LC gradient was as follows: 0–5 min, 1% B; 5–50 min, 1–35% B; 50–55 min, 35–90% B; 55–56 min, 60–90% B; 56–60 min, 90% B; 60–62 min, 90–1% B; 62–64 min, 1% B.

Peptides were sprayed into the MS through the twin sprayer ion source with the following parameters: 50 GS1, 50 GS2, 30 CUR, 5.5 keV ISVF, 450°C TEM, 80 V declustering potential and 10 V

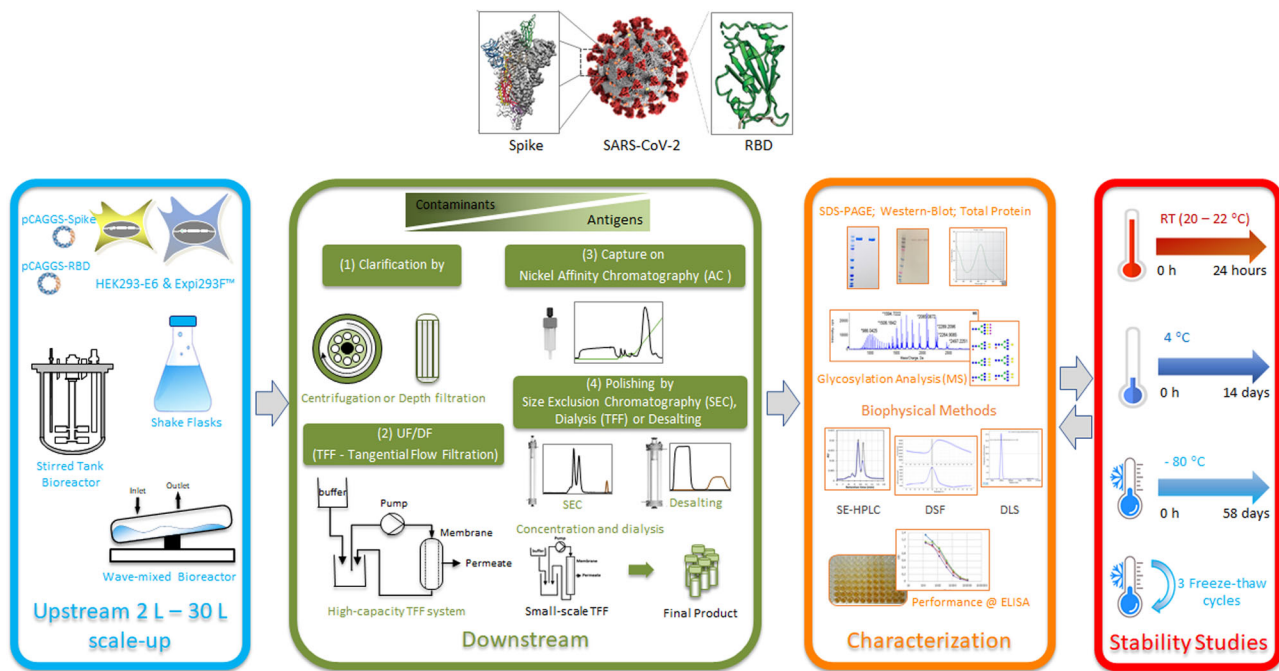


FIGURE 1 Experimental set-up for production, characterization and storage of SARS-CoV-2 Spike and RBD recombinant proteins. Top illustration of SARS-CoV-2 and Spike/RBD were adapted from Centers for Disease Control and Prevention, US (CDC ID#23311, Alissa Eckert, MSMI; Dan Higgins, MAMS, 2020) and Wrapp et al. (2020), respectively. RBD, receptor binding domain [Color figure can be viewed at wileyonlinelibrary.com]

collision energy. An information dependent acquisition method was set with a TOF-MS survey scan of 350–2000 m/z for 250 ms. The 12 most intense precursors were selected for subsequent fragmentation MS/MS mode (150–1800 m/z for 100 ms each). The selection criteria for parent ions included dynamic background subtraction and counts above a minimum threshold of 300 counts/s. Ions were excluded from further MSMS analysis for 5 s. Fragmentation was performed using rolling collision energy with a collision energy spread of 5.

MS data were analysed using the BioPharmaView software (BPV, Version 3.0, SCIEX) and the protein sequences of Spike and RBD (Amanat et al., 2020). For glycans identification, N-glycans described in Watanabe et al. (2020) were added to the BPV software database (glycans identification is provided in Table S2). Glycans were identified using MS1 data (considering a peptide deconvolution tolerance and m/z tolerance of 10 ppm) and fragmentation data when available (considering a MSMS tolerance of 0.03 Da). All MSMS data were manually examined for the presence of MSMS specific glycan marker ions. For glycans identified only with MS1, the data was also manually examined for consistence in retention time information and spectrum quality.

2.5.6 | Enzyme-linked immunosorbent assay

Anti-Spike and RBD ELISA assay implemented followed a checkerboard strategy, whereby both the antigen and the positive sera were serially titrated. The ELISA was performed as described in (Stadlbauer et al., 2020) with minor modifications. Briefly, high binding 96-well

plates (Corning) were coated with either RBD or Spike as capture antigen along a 1:2 dilution in PBS starting at 2 $\mu\text{g/ml}$, and blocked with PBS supplemented with 2% BSA. Reference positive sera were submitted to a 1:3 serial dilution starting at 1 in 50 and reference negative sera were used at 1 in 50 dilution. Bound IgG was revealed with goat anti-Human IgG Fc-HRP (Abcam) followed by incubation with 3,3',5,5'-tetramethylbenzidine (BD OptEIA™, BD Biosciences). The colorimetric assay was read at 450 nm. ELISA method standard error was determined using four independent experiments and at least, duplicate measurements of reference sera reactivity to both Spike and RBD. Reference sera were collected at least 7 days post the first PCR SARS-CoV-2 diagnostic (positive sera) or at least 3 years before the COVID-19 pandemic (negative sera). Positive and negative sera were obtained upon informed consent in the frame of the projects "Genetic susceptibility factors and immunologic protection in COVID-19," and "Genetic variance in Portuguese population: candidate genes in COVID-19," both approved by the IGC Ethic Committee (reference H004.2020 and H002.2020, respectively).

3 | RESULTS

3.1 | SARS-CoV-2 Spike and RBD production

In this study we have used two human cell lines, HEK293-E6 and Expi293F™, for the production of SARS-CoV-2 Spike and RBD. The experimental set-up is summarized in Figure 1. Different approaches for the

upstream and downstream processes were evaluated. The impact of these production strategies and scales in antigens' quality was assessed by an in-depth biochemical and biophysical characterization. Thermal stability during storage and the impact of freeze-thaw cycles was also studied. Ultimately, antigens' quality was confirmed by measuring the reactivity in ELISA COVID-19 serologic tests using human sera.

Spike and RBD bioprocess final yields, obtained after purification (mg protein per liter of culture) are presented in Figure 2a, that also shows, for comparison, data obtained from the literature (Amanat et al., 2020; Arbeitman et al., 2020; Esposito et al., 2020; Herrera et al., 2021; Johari et al., 2020; Li et al., 2020; Stuible et al., 2020).

Overall, for Spike, independently of the cell culture system (shake flasks, stirred tank or wave-mixed bioreactors) or the scale (5–30 L) used, the day of harvest is the parameter that has the highest impact in the antigens' final yields, approx. 1 and 2 mg/L culture at Day 3 and 4 posttransfection, respectively. The 1-day extension of the culture, that allows for duplication of the productivity, has not compromised neither the quality of the protein, as

assessed by SDS-PAGE and performance in the ELISA serologic tests (left panel of Figure 2b,c). Small-scale (200 ml) feasibility studies performed in shake flasks indicated that one extra day of culture, that is, harvesting at Day 5 posttransfection, led to protein degradation resulting in lower final yields (data not shown). In fact, Spike degradation was only detected for the wave-mixed bioreactor runs (Figure 2b), being more evident for the first run. Additionally, Spike produced in the first wave-mixed bioreactor run presented lower performance in SARS-CoV-2 ELISA (Figure 2c).

Similar results were obtained for RBD in what concerns the impact on protein degradation and performance at ELISA tests, that is, no significant degradation occurred for all the culture systems and scales tested and equivalent ELISA performance was observed. In fact, no degradation was detected for RBD purified from bulks harvested at Day 5 posttransfection, as assessed by SDS-PAGE (Figure 2b right panel).

For the different downstream strategies evaluated for Spike and RBD purification (see Section 2) there was no major impact in

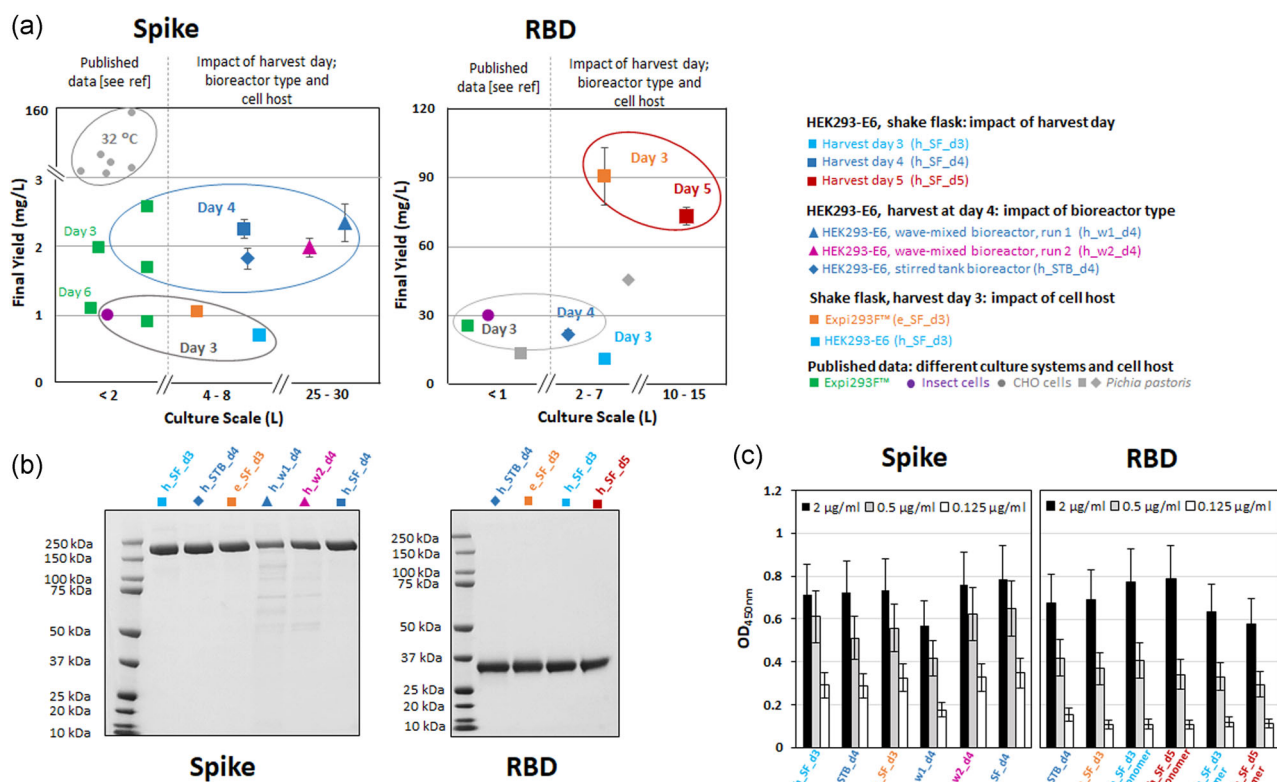


FIGURE 2 SARS-CoV-2 Spike and RBD production. (a) Impact of harvest day, bioreactor type and cell host on Spike and RBD final production yields and quality, assessed by (b) SDS-PAGE, and (c) ELISA SARS-CoV-2 positive serum reactivity. (a) Includes a comparison with data recently published in the literature (Amanat et al., 2020; Arbeitman et al., 2020; Esposito et al., 2020; Herrera et al., 2021; Johari et al., 2020; Li et al., 2020; Stuible et al., 2020). When production scale was not specified, namely for the insect and CHO cell cultures (Amanat et al., 2020; Johari et al., 2020; Li et al., 2020; Stuible et al., 2020) an assumption of <2 L was made; Error bars represent standard deviation of two measurements. (b) Three microgram of each protein was loaded per lane under reducing conditions. The results shown in (c) were obtained in ELISA plates coated with 2, 0.5, and 0.125 µg/ml of Spike or RBD (see Section 2 for details). ELISA reactivity was assessed by OD 450 nm using SARS-CoV-2 positive serum collected 14 days post PCR diagnostic and diluted 1:1350. The ELISA assay specificity was assessed by analysis of negative serum reactivity to Spike and RBD (Figure S1). Error bars represent 20% error of the ELISA method (see Section 2 for details). ELISA, enzyme-linked immunosorbent assay; PCR, polymerase chain reaction; RBD, receptor binding domain; SDS-PAGE, sodium dodecyl sulfate polyacrylamide gel electrophoresis [Color figure can be viewed at [wileyonlinelibrary.com](https://onlinelibrary.wiley.com)]

production yields. Affinity chromatography (AC), in particular the washing and elution steps, allowed for important reduction of protein impurity profile with only single bands visible in SDS-PAGE (Figure 2b). This high purity was achieved independently of performing or not the size exclusion chromatography (SEC) as polishing step.

The studies with different cell hosts, Expi293F™ and HEK293-E6, show that for similar culture conditions harvested at Day 3 posttransfection, as described in (Amanat et al., 2020), there is no significant effect in productivity for Spike. In contrast, higher yields were obtained for RBD when Expi293F™ cells were used (approx. 90 mg/L) only achieved by HEK293-E6 cells when the culture was extended two extra days (harvesting at Day 5 posttransfection, Figure 2a).

For all parameters studied, both for Spike and RBD, no significant effect was observed in the performance of ELISA serologic tests (excluding the first run of wave-mixed bioreactor); in contrary, as expected, this performance is affected by the amount of antigen used to coat the ELISA plates (Figure 2c black, gray, and white bars).

It is worth to mention that all HEK293-E6 cultures harvested after 4 days posttransfection were exhausted for glucose, in particular, the STB cultures, were depleted of glucose already at 2 days posttransfection (data not shown). In contrast, cultures of Expi293F™ cells expressing Spike or RBD had about 10 mM of glucose at harvesting time (Day 3 posttransfection) because according to the manufacturer instructions, an enhancer solution is added at 18 h posttransfection (data not shown). These results indicate the potential of further increase in protein expression yields in STB productions using HEK293-E6 cells by implementing a fed-batch operation mode with glucose supplementation.

Parallel small-scale expression screens were conducted with the ultimate goal of evaluating if the amount of coding DNA used for cell transfection and temperature shifts during production impacts antigens' production yields. The results (Figure 3) show that lowering the expression temperature to 32°C was only beneficial for Spike expression in Expi293F™, resulting in a significant increase in productivity (approx. fivefold as measured by densitometry). This productivity was further improved when the temperature shift to 32°C was combined with lowering the coding DNA amount by 50% (Figure 3 top right). For HEK293-E6 cells, no improvement in antigens' expression was obtained. Curiously, when Spike is produced at 32°C, the SDS-PAGE bands migrate slightly less, suggesting differences in Spike glycosylation profiles.

Overall, the results summarized in Figures 2 and 3 show that we were able to develop scalable bioprocesses to produce and purify at large-scale (up to 30 L) high-quality Spike and RBD antigens, maintaining or improving the production yields reported in the literature for smaller scales using human derived cell hosts (Figure 2a).

3.2 | Characterization of produced Spike and RBD

The extensive glycosylation of SARS-CoV-2 Spike protein is well described in the literature (Grant et al., 2020; Henderson et al., 2020;

Shajahan et al., 2020; Watanabe et al., 2020). In this study, we investigated Spike and RBD glycosylation patterns, focusing on putative differences between the two expression cells hosts used.

We first performed lectin blotting analysis to evaluate the presence of specific glycans in Spike and RBD samples produced in HEK293-E6 and Expi293F™ cells. All proteins were detected with SNA and MAL, which indicated the presence of α 2,6- and α 2,3-linked Neu5Ac (Figure 4). Neu5Ac was largely present in N-glycans as evaluated from decrease in signal after digestion with PNGase F (Figure S2A). As control, sensitivity to *A. urefaciens* sialidase supported the signal specificity (Figure S2A). Proteins were also detected with GNA, therefore supporting the presence of high mannose structures, particularly evident in Spike protein samples. Specificity was confirmed by a decrease in signal after digestion with Endo H (Figure S2B).

Proteins were also detected with WFA (binds terminal GalNAc), therefore, indicating the presence of the GlcNAcGalNAc (LacdiNAc) structure; this structure was present in N-glycans as inferred from PNGase F sensitivity (Figures 4 and S2C). Proteins were also strongly detected with AAL (Figure 4), which indicated proximal fucosylation and possibly peripheral fucosylation.

Spike and RBD have 22 and 2 potential N-glycosylation sites, respectively. We have performed LC-MS analysis to screen for the presence of N-glycans previously identified by others in SARS-CoV-2 Spike protein (Watanabe et al., 2020). A detailed description of the different glycoforms detected in each site from tryptic peptides of Spike and RBD produced in HEK293-E6 cells and Expi293F™ cells is presented in Supplementary data (Files "Glycans comparison" and "MS data").

To investigate site-specific glycosylation and differences between HEK293-E6 and Expi293F™ cells comparison of N-glycan

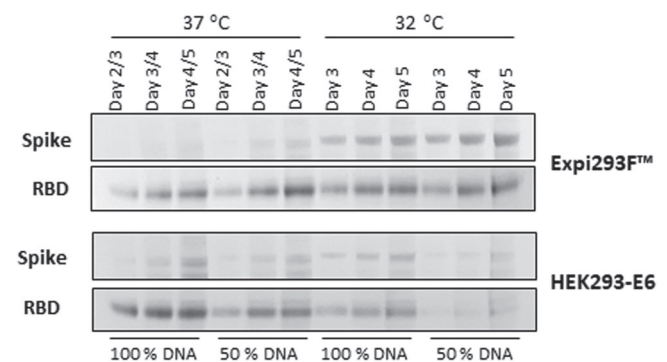


FIGURE 3 Effect of temperature shift and coding DNA amount on Spike and RBD production. Reducing SDS-PAGE analysis of Expi293F™ or HEK293-E6 culture supernatants expressing Spike and RBD at 32°C or 37°C, after transfection with 1 μ g coding DNA/ml (100%) or 0.5 μ g coding DNA/ml (50%). A total of 20 μ l of Spike expressing culture supernatants were loaded in each lane. A total of 5 and 10 μ l of RBD supernatants from Expi293F™ and HEK293-E6 cultures, respectively, were loaded in each lane. Spike and RBD expression at 37°C was analysed from Day 3 to 5 posttransfection in HEK293-E6 cultures or Day 2 to 4 posttransfection in Expi293F™ cultures. RBD, receptor binding domain; SDS-PAGE, sodium dodecyl sulfate polyacrylamide gel electrophoresis

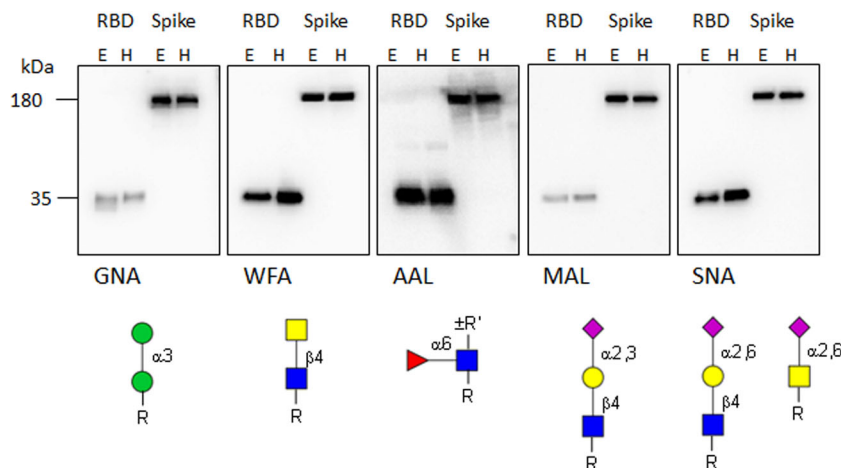


FIGURE 4 Effect of host cell in lectin blotting of Spike and RBD. RBD produced in Expi293F™ cells (E) or HEK293-E6 cells (H) and Spike produced in Expi293F™ cells (E) or HEK293-E6 cells (H) have been detected with the lectins GNA, WFA, AAL, MAL, and SNA. Each lane contained 200 ng protein. Preferred glycan specificities of lectins are shown and are according to the suppliers and to the literature (Cummings et al., 2017). Glycan representation is according to the Consortium of Functional Glycomics. Results are representative of at least 3 blots. AAL, *Aleuria aurantia* lectin; GNA, *Galanthus nivalis* agglutinin; MAL, *Maackia amurensis* lectin; RBD, receptor binding domain; SNA, *Sambucus nigra* agglutinin; WFA, *Wisteria floribunda* agglutinin [Color figure can be viewed at wileyonlinelibrary.com]

compositions was also done (Supporting Information File “Glycans comparison”). For a qualitative evaluation, structures (compatible with the monosaccharide compositions, the N-glycan biosynthetic pathway and the lectin blotting above) have been proposed using GlycoWorkbench (Ceroni et al., 2008; Table S2). Glycoforms of each identified site from Spike and RBD, produced either in HEK293-E6 or Expi293F™ cells, were compared based on the following structural features: presence of high mannose glycans, fucosylation (proximal and peripheral), sialylation, sialylation and fucosylation and detection of sialyl-LacdiNAc (Tables 1 and 2).

SARS-CoV-2 Spike and RBD from the two host cells displayed high mannose, paucimannose, hybrid and complex di-, tri-, and tetra-antennary glycans. Many fucosylated structures were detected, which included proximal fucose and also peripheral fucose (the latter inferred from the presence of more than one fucose residue in glycan compositions, e.g., structures 47, 72, 81, etc). Complex glycans were partially or completely sialylated. The proteins bound the lectin WFA (Figure 4), which indicated the presence of LacdiNAc, compatible with proposed structures 49, 50, 52–54, 56, 57, 77, 78, 80–82, 86–89, 91, and 107–109. The presence of LacdiNAc was further supported by the unequivocal finding of sialylated LadiNAc in structures 27, 51, 55, 59, 79, and 90. It should be considered that bisecting GlcNAc-containing structures are also compatible with the detected masses (Table S2).

Glycoform profiles of individual Spike sites were quite distinct. Most striking was: the abundance of high mannose glycans at N234, low heterogeneity at N17 with a relatively high proportion of hybrid and paucimannose structures but undetectable high mannose structures; high heterogeneity at sites N61/N74 and N331/N343 (which could be attributed to the presence of two N-glycosylation sites in the same tryptic peptide).

When Spike glycoform profiles were compared between host cells some differences were found, but not striking (Table 1;

Supporting Information Files “Glycans comparison Spike samples”). On the other hand, for RBD glycoforms, which has only two N-glycosylation sites (N331 and N343 both present in the same tryptic peptide), a remarkable difference was found between HEK293-E6 cells and Expi293F™ cells derived protein (Table 2). The heterogeneity was very high in RBD produced in HEK293-E6 cells, with the detection of large high mannose glycans ($\text{Man}_9\text{GlcNAc}_2$ and $\text{Man}_8\text{GlcNAc}_2$) and several sialylated/fucosylated complex glycans. By contrast RBD produced in Expi293F™ cells exhibited fewer glycoforms, which included the small high mannose glycan ($\text{Man}_5\text{GlcNAc}_2$), several paucimannose/hybrid structures, and fewer complex sialylated/fucosylated glycans.

Besides the analysis of Spike and RBD glycosylation profile, we also proceeded with the assessment of overall oligomeric state of the proteins. SARS-CoV-2 Spike forms trimers that interact with ACE2 receptor at the RBD region (Esposito et al., 2020; Walls et al., 2020; Wrapp et al., 2020). We have started by performing size-exclusion HPLC analysis of Spike protein in a Xbridge BEH200 column. The results indicated that Spike has a molecular weight of approximately 600 kDa, confirming its trimeric conformation (Figure 5a). Since we were interested in evaluating the presence of protein aggregates, we have run Spike samples in a Xbridge BEH450, an SE-HPLC column suitable for the analysis of high-molecular weight proteins (Figure 5b). Unexpectedly, the Spike peak was resolved into two separated peaks eluting at 9.7 and 10.8 min, that corresponded to apparent molecular weight of approximately 1200 and 600 kDa, respectively. This elution profile was present in all Spike samples, produced in HEK293 or Expi293F™ cells, in shake flask, stirred tank or wave-mixed bioreactors, although the relative contribution of each Spike peak changed (data not shown). A small peak of putative aggregates was also detected in all Spike samples at retention time of approximately 8.5 min (Figure 5b).

Glycan	N17		N61 N74		N122		N149		N165		N234		N282		N331 N343		N798		N1071		N1095		N1170		N1191			
	H	E	H	E	H	E	H	E	H	E	H	E	H	E	H	E	H	E	H	E	H	E	H	E	H	E		
60																												
61																												
62																												
63																												
64																												
65																												
66																												
67																												
68																												
69																												
70																												
71																												
72																												
73																												
74																												
75																												
76																												
77																												
78																												
79																												
80																												
81																												
82																												
83																												
84																												
85																												
86																												
87																												
88																												
89																												
90																												
91																												
92																												
93																												
94																												
95																												
96																												
97																												
98																												
99																												
100																												
101																												
102																												
103																												
104																												
105																												
106																												
107																												
108																												
109																												

Note: Results were obtained with Spike samples from shake flask cultures harvested at Day 3 posttransfection, using HEK293-E6 (H) or Expi293F™ cells (E). MS data were screened considering the 109 N-glycans structures previously identified in SARS-CoV-2 Spike (Watanabe et al., 2020; Table S2). Colors represent the following N-glycans structural features: high mannose (green), fucosylated (red), sialylated (purple), sialylated/fucosylated (dark gray), sialyl-LacdiNac (yellow), and others (light gray).

TABLE 2 Comparison of glycan composition in RBD produced in HEK293-E6 or Expi293F™ cells

	H	E		H	E		H	E		H	E		H	E
1	Green		23	Light Gray		45	Dark Gray		67			89	Dark Gray	
2	Green		24			46	Red		68	Red	Red	90		
3			25	Red	Red	47	Red		69			91	Red	
4			26	Red		48			70			92	Light Gray	
5		Green	27	Yellow		49	Light Gray		71			93	Red	
6		Light Gray	28	Light Gray		50	Red	Red	72	Red		94		
7		Red	29	Red	Red	51	Yellow		73			95		
8		Light Gray	30	Dark Gray		52	Light Gray		74			96	Red	
9		Red	31	Red		53	Red		75	Purple		97	Red	
10	Purple		32	Purple		54	Dark Gray		76	Purple		98		Light Gray
11			33			55	Yellow		77			99	Red	
12	Red		34	Red	Red	56	Red		78	Red	Red	100		
13			35	Dark Gray		57			79	Yellow		101		
14			36	Dark Gray		58	Purple	Purple	80		Red	102		
15		Light Gray	37			59	Yellow		81	Red		103		
16		Red	38			60	Light Gray		82	Light Gray		104		Purple
17		Light Gray	39	Red		61	Red		83	Red		105		
18		Red	40			62	Dark Gray		84	Red		106		
19		Light Gray	41	Purple		63	Dark Gray		85	Purple		107	Red	
20		Red	42	Purple		64	Red		86			108	Light Gray	
21			43	Light Gray		65	Red		87	Red		109	Red	
22			44			66	Purple		88	Dark Gray				

Note: Results were obtained with RBD samples from HEK293-E6 stirred tank bioreactor culture harvested at Day 4 posttransfection (H) or Expi293F™ shake flask culture harvested at Day 3 posttransfection (E). MS data was screened considering the 109 N-glycans structures previously identified in SARS-CoV-2 Spike (Watanabe et al., 2020; Table S2). Colors represent the following N-glycans structural features: high mannose (green), fucosylated (red), sialylated (purple), sialylated/fucosylated (dark gray), sialyl-LacdiNac (yellow), and others (light gray).

Analysis of RBD by size exclusion HPLC validated the observations performed during RBD purification runs. Interestingly, RBD production in HEK293-E6 cells resulted in a mixture between RBD monomer and dimer, with up to 45% of dimer, whereas in Expi293F™ production run, 93% of RBD is in monomeric state (Figure 5c).

3.3 | Spike and RBD thermal stability

The ultimate goal of this study is to develop scalable bioprocess to produce and supply high-quality antigens to prepare SARS-CoV-2 ELISA serology assays. Considering that automation will be needed for ELISA plates preparation and that its global distribution will be required, it is critical to evaluate Spike and RBD thermal stability, namely during storage and when subjected to freeze-thaw cycles. We have analyzed Spike and RBD thermal denaturation by DSF (Figure 6 and Table S1). Spike presented a melting temperature of 44.7°C, whereas RBD shows slightly improved thermal stability, with a melting temperature of 49.4°C. Additionally, RBD produced in Expi293F™ presented slightly increased melting temperature as compared to the RBD produced in HEK293-E6 cells (Table S1). All Spike samples analyzed, independently of cell host or cell culture process, presented the same melting temperature, as assessed by nanoDSF (Table S1).

Size exclusion HPLC was used to investigate the impact of temperature during storage on Spike and RBD conformation. Antigens obtained from STB runs (HEK293-E6 cells), were incubated at 4°C or at

room temperature (RT, 20°C–22°C), up to 14 days or 24 h. Analysis of Spike and RBD during storage at –80°C was also performed for up to 58 days.

For Spike, we observed conversion between SEC species when incubated at 4°C or RT (Figure 7a). After 24 or 6 h at 4°C or RT, respectively, only one peak was detected at approximately 9.7 min. During storage at –80°C, the proportion between SEC species is comparable for up to 58 days. Putative Spike aggregates were also detected in all conditions and accounted for up to 10% of total SEC species during incubation of Spike at 4°C or during storage at –80°C, or up to 20% after 6 h of incubation at RT (data not shown). The conversion between SEC species described for Spike protein was also observed for Spike produced in Expi293F™ cells, when incubated at 4°C (data not shown).

Analysis of RBD samples after incubation at 4°C, RT or during storage at –80°C, showed that the monomer/dimer moieties were maintained in all conditions (Figure 7b). Likewise, the monomeric portion of RBD, when produced in Expi293F™ cells, was maintained up to 14 days at 4°C (data not shown).

Importantly, our results show that performing 3 freeze-thaw cycles to either Spike or RBD did not result in significant changes in the antigens' conformation or oligomeric state (Figure 7).

Moreover, no protein degradation was detected by SDS-PAGE when samples of Spike and RBD were analyzed after 14 days at 4°C or, only for Spike, after 24 h incubation at RT (data not shown).

DLS analysis was also performed to further investigate the impact of temperature in Spike and RBD proteins (Table 3). The polydispersity index (PDI) determined for Spike samples ranged from 13% to 20% and

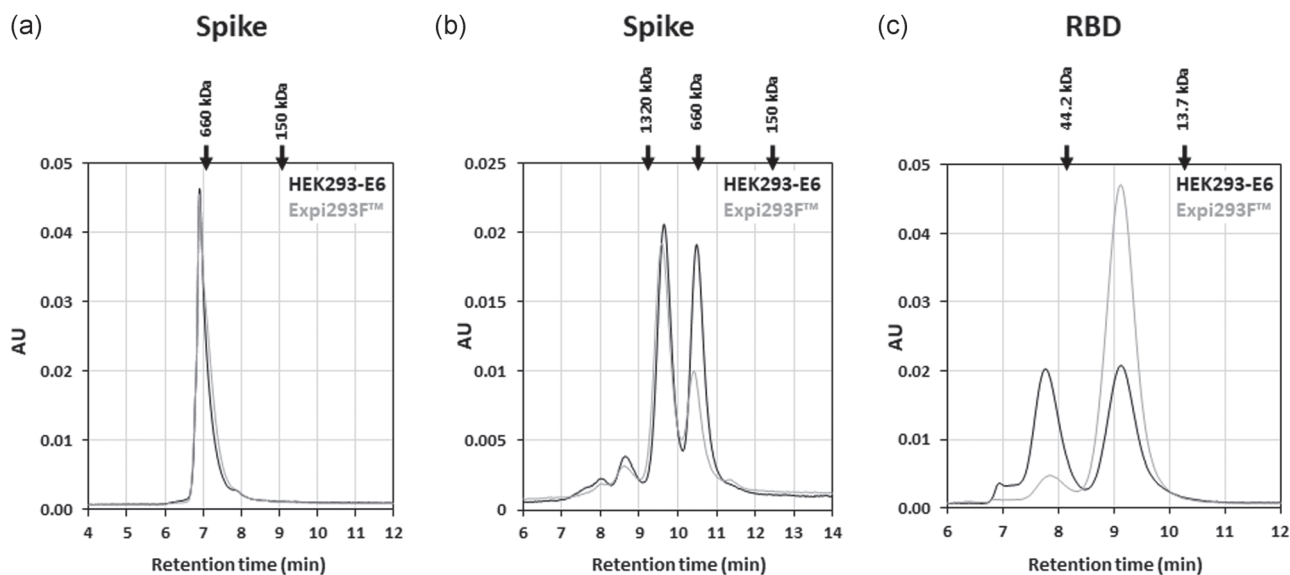


FIGURE 5 Effect of host cell in Spike and RBD oligomeric state. Size-exclusion HPLC analysis of Spike (a, b) and RBD (c) purified proteins produced in Expi293F™ and HEK293-E6 cells. Spike samples were analysed with Xbridge BEH200 (a) or Xbridge BEH450 (b) HPLC columns and RBD samples were analysed in Xbridge BEH125 column (c). Protein standard mixes were injected in each column, under the same conditions, and the arrows indicate the respective retention time. Protein standards used: thyroglobulin dimer (1320 kDa), thyroglobulin (660 kDa), IgG (150 kDa), ovalbumin (44.2 kDa), and ribonuclease A (13.7 kDa). HPLC, high-performance liquid chromatography; RBD, receptor binding domain

the estimated molecular weight was approximately 600–700 kDa, a value in agreement with the expected size of glycosylated Spike trimer. No major differences in PDI or molecular weight were observed for the several Spike sample treatments or for the different Spike tested (from HEK293-E6 productions in stirred tank or wave-mixed bioreactors and Expi293F™ productions). Most of the RBD results presented in the table are relative to the protein obtained from STB cultures, which consist of a quasi-equi-molar mixture of RBD monomer and dimer. These samples presented PDI between 24% and 35% and estimated molecular weight

around 70 or 120 kDa, higher than the expected molecular weight of either RBD monomer or dimer. When RBD was subjected to three freeze-thaw cycles, two particles of different sizes were detected (Table 3). Lower PDI of 11–18% and lower estimated molecular weight around 40 kDa were determined for RBD monomer samples, obtained from Expi293F™ or HEK293-E6 productions.

The observation that Spike undergoes putative conformational changes when incubated at 4°C or RT (Figure 7), raises the question whether these changes impact the performance of Spike as antigen

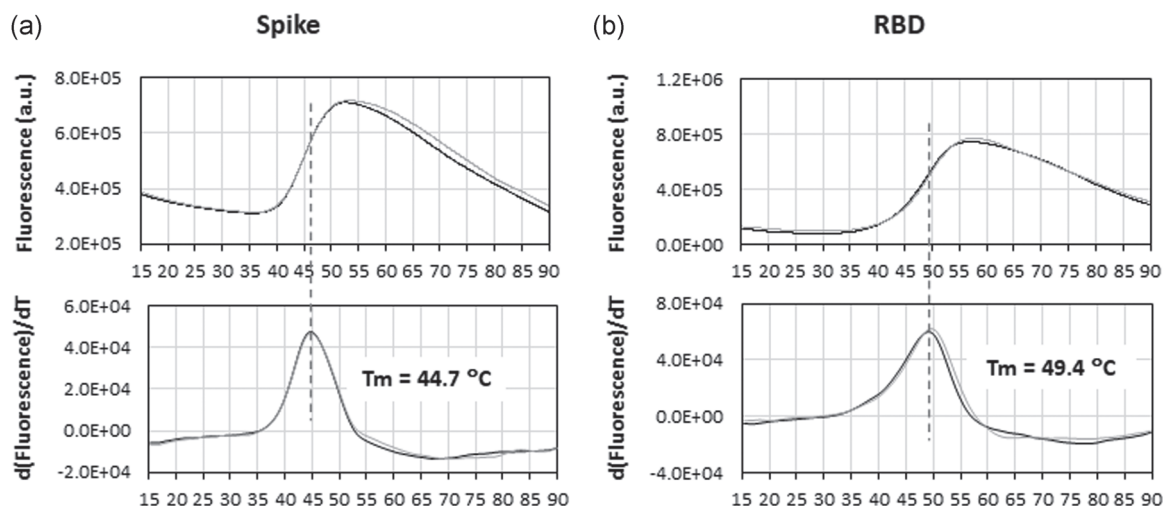


FIGURE 6 Spike and RBD thermal stability. Differential scanning fluorimetry analysis of Spike produced in stirred tank bioreactor (h_STB_d4) using HEK293-E6 cells and RBD monomer sample produced in HEK293-E6 shake flask culture harvested at Day 5 posttransfection (h_SF_d5 monomer). The average melting temperature was determined considering the two replicate measurements shown in the figure. RBD, receptor binding domain

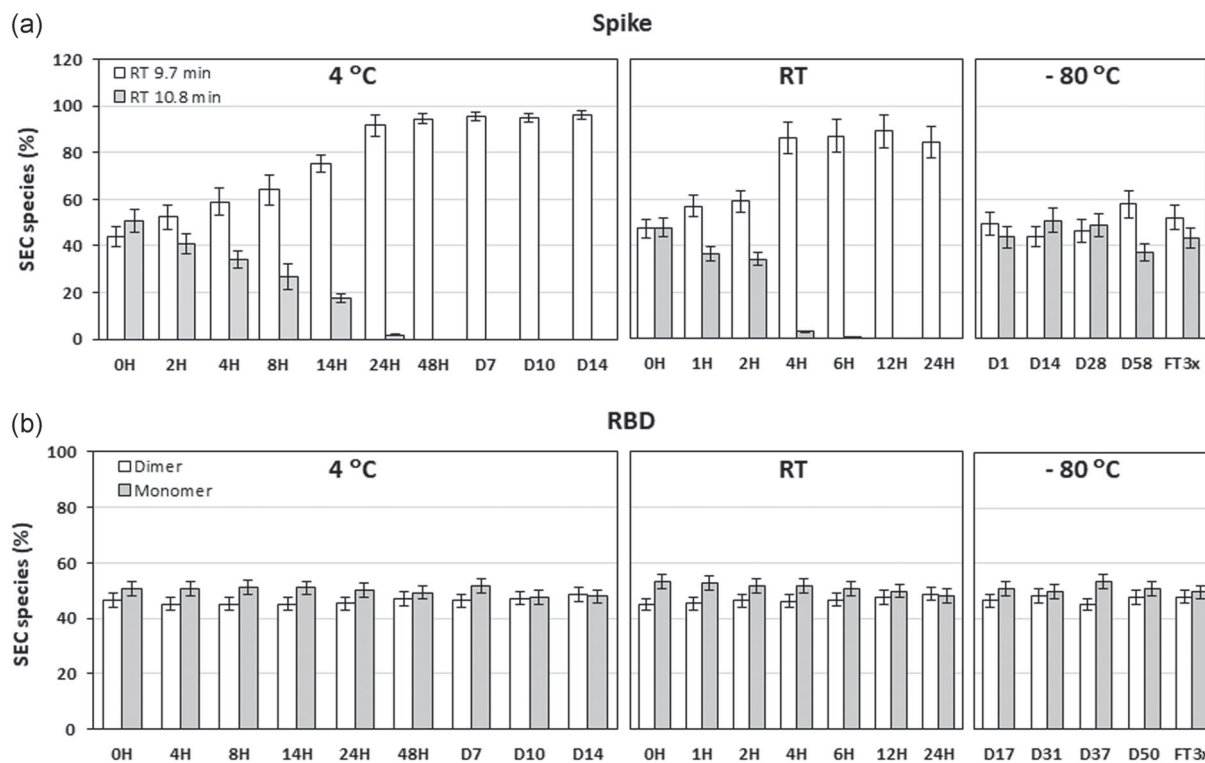


FIGURE 7 Impact of storage temperature on Spike and RBD conformation. Size-exclusion HPLC analysis of Spike protein using Xbridge BEH450 (a) or RBD protein using Xbridge BEH125 (b). Results were obtained with the Spike and RBD produced in HEK293-E6 stirred tank bioreactor cultures harvested at Day 4 posttransfection (h_STB_d4). Protein samples were stored at 4°C, RT or at -80°C, for several time-points. The starting point of the analysis (0 h) consists in injecting the sample into HPLC column immediately after thawing from -80°C. Samples FT3x were subjected to three freeze-thaw cycles using liquid nitrogen. The error of two measurements is represented in bars. HPLC, high-performance liquid chromatography; RBD, receptor binding domain

for the detection of SARS-CoV-2 specific antibodies. Therefore, we performed ELISA assays using as plate coating Spike and RBD samples after incubation at 4°C, RT or after freeze-thaw cycles. The results show that the serum reactivity to both antigens, as well as the assay specificity, was maintained despite the treatments performed (Figures 8 and S3). Furthermore, the data reveals good reproducibility for Spike samples coated at different antigen concentrations, whereas for RBD, coating at low concentration of 0.125 µg/ml increases the ELISA serology test variability.

4 | DISCUSSION

COVID-19 pandemic triggered a combined and global effort of the scientific community to understand the new SARS-CoV-2 virus and its key players during infection. Thus, a worldwide demand for SARS-CoV-2 proteins was launched. Spike protein, being responsible for the binding to the ACE2 receptor, and consequently for the virus entry in the host cells, has been intensively studied and is one of the most clinically relevant SARS-CoV-2 proteins. In this study, we have studied the production of full-length Spike and its RBD using human derived cell lines, with the intention of applying the two Spike protein formats as antigens in SARS-CoV-2 serological assays.

We showed that, for both Spike and RBD productions, the yields obtained with HEK293-E6 cells, using regular transfection reagents and protocols (Durocher et al., 2002), were in the same order of magnitude of those obtained with highly improved Expi293F™ expression system (Figure 2a; Amanat et al., 2020; Esposito et al., 2020; Herrera et al., 2021). Additionally, we shown that equivalent final Spike production yields could be obtained for the three different cell culturing strategies tested: shake flask, stirred tank, and wave-mixed bioreactors, with production scales ranging from 2 L up to 30 L. By analyzing the media metabolites through the culture time (data not shown) we anticipate that Spike and RBD production yields can be further improved in HEK293-E6 cultures by the implementation of feeding strategies consisting mainly in glucose refeeds (Jäger et al., 2015; Pham et al., 2005; Stuble et al., 2020). Performing such feed would be of particular importance in STB cultures, since we observed early glucose depletion (data not shown).

Aiming at decreasing the antigens DSP time and reducing protein losses with unnecessary purification steps we evaluated the impact of process adjustments on final product purity and ultimately on the antigen performance in SARS-CoV-2 specific ELISA assays. The polishing step by SEC could be replaced by dialysis or desalting steps without impacting overall antigen quality, the same conclusion was recently published by other groups (Esposito et al., 2020;

TABLE 3 Dynamic Light Scattering analysis of Spike and RBD

Condition		Spike		RBD	
		PDI (%)	MW (kDa)	PDI (%)	MW (kDa)
-80°C (HEK293-E6)	D2	14.7	581	23.9	111
	D30	17.1	657	35.2	154
	D44 (monomer)	-	-	10.9	41
	D1 (wave)	20.4	751	-	-
-80°C (Expi293F™)	D1	19.6	695	-	-
	D57	-	-	18.4	48
4°C (HEK293-E6)	40 h ^a	13.3	630	32.4	139
	D7	14.1	617	-	-
	D14	15.1	701	26.5	79
	16 h ^a (wave)	19.2	732	-	-
3x Freeze-thaw (HEK293-E6)		15.8	641	10.5/ 29.8 ^b	74/ 158 ^b

Note: Results were obtained with Spike and RBD samples from HEK293-E6 stirred tank bioreactor cultures (h_STB_d4) and Expi293F™ shake flask cultures (e_SF_d3), RBD monomer from HEK293-E6 shake flask culture harvested at Day 5 posttransfection (h_SF_d5) and Spike from second wave-mixed bioreactor production using HEK293-E6 cells (h_w2_d4).

^aSamples analyzed without fast freezing in liquid nitrogen.

^bTwo species detected by DLS.

Herrera et al., 2021; Stadlbauer et al., 2020). Moreover, the protocol established for product elution from affinity chromatography allowed for the achievement of high-purity products, with only one purification step (Figures 2b and 5). Additionally, Spike and RBD purity, oligomeric state, thermal stability and performance on ELISA assays, were similar for the different lots produced (Figure 2b,c; Table 3 and S1). The only exception being the Spike produced in the first run of wave-mixed bioreactor, that presented slightly lower reactivity to SARS-CoV-2 positive serum as assessed by ELISA (Figure 2c). This lower performance on ELISA test is most likely the result of Spike degradation, as observed in SDS-PAGE (Figure 2b) and this Spike protein degradation was likely due to extended DSP times. Therefore, we implemented changes in the DSP of large-scale production batches that would, not only reduce processing time, as also allow for further scaling-up of antigen production process in an industrial setup. On the subsequent Spike production using wave-mixed bioreactor, we bypassed large-scale culture centrifugation by using high-capacity filters to clarify culture bulk, and the final SEC step was replaced by sample dialysis. The overall processing time was reduced, and analysis of resulting Spike lot suggested lower degree of protein degradation and undistinguishable SARS-CoV-2 positive serum reactivity to Spike, as compared to Spike from smaller production scales (Figure 2b,c).

Transient gene expression using mammalian cells has been established for decades (Baldi et al., 2012; Durocher et al., 2002;

Nettleship et al., 2010; Pham et al., 2006). Several approaches have been described for the improvement of transient protein expression, in particular for difficult-to express proteins (Estes et al., 2015; Lin et al., 2015; Mason et al., 2014; Simone et al., 2003), namely decreasing both the expression temperature and coding DNA amount. We obtained a significant improvement of Spike expression in Expi293F™ cells when the cell culture temperature was reduced to 32°C (Figure 3), also in agreement with recently published data for SARS-CoV-2 Spike protein production in the same cells (Esposito et al., 2020; Herrera et al., 2021). Additionally, we show that combining temperature decrease and reduction of coding DNA concentration to 50% further improves Spike production in Expi293F™ cells. Surprisingly, in HEK293-E6 cells, decreasing of temperature to 32°C had only marginal effects on Spike expression (Figure 3) suggesting that other parameters may be limiting Spike expression. One can speculate that the lack of a carbon source, as discussed above, might be the reason that can be overcome by implementing fed-batch strategies combined with a fine tune of temperature and DNA shifts. In fact, recent studies report high titers of Spike expression when using CHO cells and optimized production protocols that combine glucose feedings, hypothermia and modulation of coding DNA amounts, among other parameters (Figure 2a; Johari et al., 2020; Stuibler et al., 2020). However, to the best of our knowledge, the impact of these optimization production strategies in the antigen's quality, namely on posttranslational modification, was not deeply discussed.

The expression screen performed showed that reduction of expression temperature or coding DNA did not improve RBD expression in either Expi293F™ or HEK293-E6 cells. Spike and RBD thermal stability analysis by DSF showed 5°C difference in the calculated protein melting temperatures (T_m), with Spike displaying lower temperature stability (Figure 6). We hypothesize that the improvement of Spike expression at 32°C in Expi293F™ cultures, is due to not only to changes in the cell metabolic state but also to improved Spike stability during expression.

Altogether, the protocols reported herein for Spike and RBD production, that range from shake flask cultures to large-scale bioreactors, can be easily implemented in academic laboratories, in clean rooms in health centers or in large-scale industrial setups.

To better understand the impact of cell hosts and bioprocess in antigen's quality and performance in ELISA serology tests a deep characterization analysis was performed. One of the main quality attributes of reagents destined to COVID-19 diagnosis and, most importantly, COVID-19 prophylaxis and therapeutics, is the human-derived post-translational modifications, that should closely mimic the natural host for SARS-CoV-2 replication. Using complementary glycomics approaches with lectin blotting and LC-MS, we showed that Spike and RBD produced in HEK293-E6 and Expi293F™ cells contained high mannose and complex glycans with proximal and peripheral fucose, α 2,3- and α 2,6-linked sialic acid, LacdiNAc and sLacdiNAc. The N-glycosylation of protein S ectodomain (Watanabe et al., 2020) and S1/S2 subdomains (Shajahan et al., 2020) produced in HEK293 cells has recently been described in the literature, where a large diversity of high mannose, hybrid and complex structures were assigned to individual sites. Here, we further identify

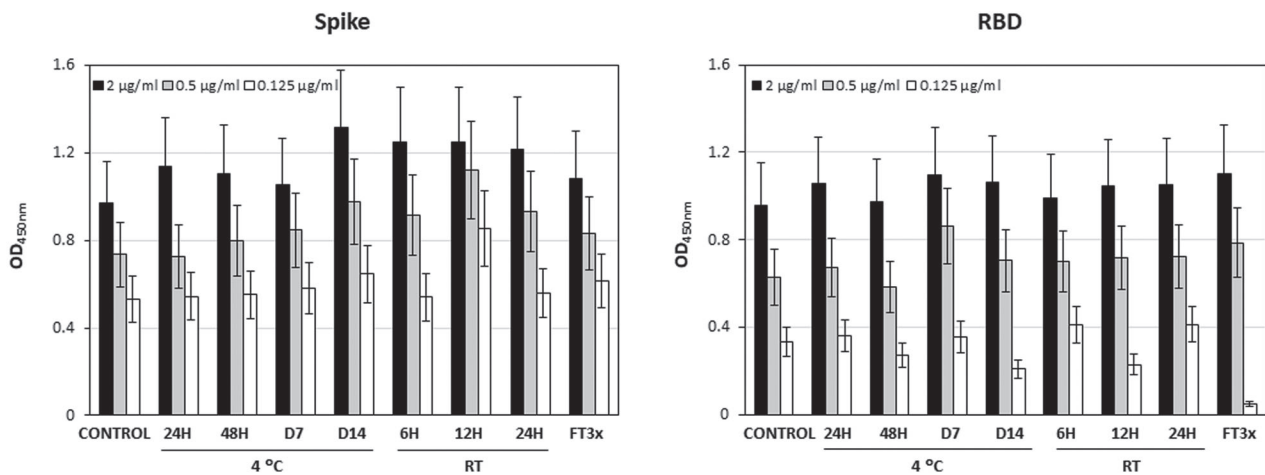


FIGURE 8 Effect of storage temperature on SARS-CoV-2 Spike and RBD performance in ELISA serologic tests. Evaluation of SARS-CoV-2 positive serum reactivity to Spike and RBD samples after incubation at 4°C, RT, or after three freeze-thaw cycles using liquid nitrogen (FT3x). Results were obtained with Spike and RBD produced in HEK293-E6 stirred tank bioreactor cultures harvested at Day 4 posttransfection (h_STB_d4). Control condition corresponds to coating the antigen after thawing from -80°C. Serial dilutions of positive serum and antigen were analysed; the data presented correspond to SARS-CoV-2 positive serum collected 25 days post PCR diagnostic diluted 1:1000 and Spike or RBD coating with 2, 0.5, and 0.125 µg/ml. The assay specificity was assessed by analysis of negative serum reactivity to Spike and RBD samples (Figure S3). Error bars represent 20% error of the ELISA method (see Section 2 for details). ELISA, enzyme-linked immunosorbent assay; PCR, polymerase chain reaction; RBD, receptor binding domain

LacdiNAc/sialyl-LacdiNAc structures and the type of sialic acid linkage. In agreement, LacdiNAc has already been detected in HEK293 cells (André et al., 2007; Costa et al., 2018) and a possible positive impact of this structure on the pharmacokinetics of recombinant proteins has been advanced (Chin et al., 2019). Furthermore, α 2,3/6-linked sialic acid has been detected in HEK293 cells N-glycans (Costa et al., 2018); sialylation has a recognized impact in the in vivo half-life of therapeutic proteins.

Only few reports have addressed the N-glycosylation properties of Expi293F™ cells (González-Feliciano et al., 2020). Since they are derived from the HEK293 cell line they would be expected to share glycosylation properties as we report here. Curiously, the N-glycosylation of RBD produced in Expi293F™ shake flask cultures showed lower diversity and a tendency towards smaller glycans ($\text{Man}_5\text{GlcNAc}_2$, paucimannose, hybrid, and partially processed glycans) in comparison to RBD produced in HEK293-E6 cells in STB (Table 2). These differences may be related to the host cell or to the production strategy used. Additionally, the slightly improved thermal stability observed for RBD produced in Expi293F™ cells (Table S1) could be a consequence of the different glycosylation profile since it is known that glycans interact with protein surface and may play a role in its stabilization. Glycan size is also particularly relevant since smaller glycans increase the accessible protein area for antibody development. Indeed, it has been recently reported that paucimannose N-glycans (e.g., $\text{Man}_3\text{GlcNAc}_2$) shield lower area at the surface of the protein than high mannose $\text{Man}_5\text{GlcNAc}_2$ or unsialylated proximally fucosylated diantennary glycan (Grant et al., 2020). Moreover, similar SARS-CoV-2 positive serum reactivity was observed for all RBD samples despite the glycosylation heterogeneity found. In contrast to RBD, glycosylation profiles of individual sites in Spike protein showed more resemblances between HEK293-E6 and Expi293F™ cells (Table 1). Most sites of Spike protein displayed a high heterogeneity, but in some cases a

tendency could be found. For example, N234 displayed predominantly high mannose glycans similarly to the reported before, which could be due to lower accessibility during glycan processing, in contrast to predominance of more processed glycoforms in accessible and loop regions (Watanabe et al., 2020). Glycosylation heterogeneity may be relevant in interactions between glycans and the protein surface, whereas glycosylation at the RBD and adjacent regions is expected to play a role in binding to the ACE2 receptor.

HPLC analysis of Spike protein using Xbridge BEH450 column showed two main forms of Spike protein, eluting at 9.7 and 10.8 min, which corresponds to apparent molecular weight of approximately 1200 and 600 kDa, respectively (Figure 5b). This particular Spike elution profile has been recently reported and most likely reflects differences in Spike conformation, rather than oligomerization (Herrera et al., 2021). Moreover, our DLS analysis together with literature data corresponding to the same Spike protein construct in the same buffer conditions, substantiates Spike's trimeric form with approximately 600 kDa (Table 3; Esposito et al., 2020; Herrera et al., 2021). The melting temperature determined for Spike and RBD are in agreement with literature data and suggest low temperature stability for both proteins, in particular for full-length Spike protein (Figure 6; Herrera et al., 2021; Li et al., 2020). So, we set out to study the impact of temperature on Spike and RBD conformation (Figure 7). Interestingly, we show here that temperature disturbs the equilibrium between the two forms of Spike detected. Time-course analysis of Spike protein after storage at 4°C or at RT showed interconversion between the two HPLC peaks (Figure 7a). This interconversion between Spike forms after 14 days storage at 4°C has also been described recently (Herrera et al., 2021).

We performed DLS analysis to further characterize Spike and RBD samples and to investigate the impact of storage at 4°C on both

proteins. The PDI obtained for Spike samples is higher than that typically obtained for monodispersed proteins (usually below 10%) (Table 3). This is not surprising taking into consideration the high degree of glycosylation detected for Spike samples (Table 1). Similar DLS results on PDI and estimated molecular weight were obtained for either different Spike samples or after sample treatment (storage at 4°C and performing three cycles for freeze-thaw). This suggested that sample treatment did not impact Spike protein. Likewise, storage of RBD at 4°C or performing freeze-thaw cycles, did not cause changes in the sample polydispersity nor in estimated molecular weight, as assessed by DLS (Table 3). Nevertheless, analysis of different RBD samples, constituted of different monomer/dimer proportions, showed differences in PDI and estimated molecular weight. Homogeneous RBD monomer samples, from either HEK293-E6 or Expi293F™ productions, presented lower PDI and lower estimated molecular weight as compared to RBD lot with equimolar contribution of dimer and monomer. Moreover, the PDI values between 24% and 35% observed for RBD produced in HEK293-E6 STB cultures, correlates well with the high degree of glycosylation detected for this sample (Tables 2 and 3).

Taking into consideration the large-scale production of ELISA tests for the detection of SARS-CoV-2 specific antibodies, most likely with the use of automated equipment to prepare the ELISA plates, together with plate storage and wide-range distribution, it is anticipated that the antigen proteins will be exposed to temperature fluctuations. So, in this study we have evaluated the performance of Spike and RBD samples as antigens in SARS-CoV-2 specific ELISA assays, after incubation at 4°C or RT, or after performing three cycles of freeze-thaw (Figure 8). Our results clearly showed that the reactivity of Spike and RBD samples to SARS-CoV-2 positive serum was maintained despite the treatments performed. In summary, our work shows that different culturing approaches can be used for scalable production in Expi293F™ or HEK293-E6 cells of SARS-CoV-2 Spike and RBD, without impacting the final production yield nor compromising the performance of ELISA serologic COVID-19 tests. Moreover, our profound analysis of Spike and RBD glycosylation contributes to the advance of current knowledge of SARS-CoV-2 Spike glycosylation patterns critical for the design and development of therapeutics to fight COVID-19. Finally, we have performed a thorough characterization of Spike and RBD in terms of thermal stability and we have shown that Spike and RBD performance as antigens in ELISA assays is maintained even after suffering from temperature fluctuations. These data are also relevant to aid industrial set-ups that will use these antigens for production of ELISA serologic tests or to supply R&D pipelines for drug discovery.

It is our believe that the results described herein are relevant for the scientific community, both in academic and industrial settings and contribute to the current knowledge of SARS-CoV-2 proteins supporting the research and clinical programs to find solutions for COVID-19 pandemics.

ACKNOWLEDGEMENTS

This study was developed within the scope of the Serology4COVID consortium, Portugal. The authors thank Florian Krammer from

Icahn School of Medicine at Mount Sinai (New York, USA), for useful discussions and for kindly supply of Spike and RBD plasmids, and patients and healthy volunteers for providing SARS-CoV-2 positive and negative serum. Ana Barbas, Cristina Peixoto, Pedro Cruz and António Roldão are acknowledged for useful discussions, and Tiago Nunes, Inês Santos and Katia Ribeiro-de-Jesus are acknowledged for their support in some experiments. We thank Sartorius BBI for proving an extra wave-mixed bioreactor (Biostat® Cultibag RM). Mass Spectrometry data presented was obtained by the UniMS – Mass Spectrometry Unit, ITQB/IBET, Oeiras, Portugal. The authors thank the financial support provided by Oeiras City Council, Portugal. The authors also acknowledge iNOVA4Health Research Unit.

CONFLICT OF INTERESTS

The authors declare that there are no conflict of interests.

AUTHOR CONTRIBUTIONS

Rute Castro and Paula M. Alves conceived the experimental design and coordinated the study. Rute Castro, Lígia S. Nobre, Rute P. Eleutério, Mónica Thomaz, António Pires, Sandra M. Monteiro, Sónia Mendes, João J. Clemente, Marcos F. Q. Sousa, Filipe Pinto, and Ana C. Silva performed the experiments related with antigens production, purification, most of the analytics and the stability during storage studies. Antigens biophysical characterization was done by Rute P. Eleutério, Micael C. Freitas, Ana R. Lemos, and Tiago M. Bandeiras. Ricardo A. Gomes, Júlia Costa, and Patricia Gomes-Alves performed the mass spectrometry and glycans analysis. Onome Akpogheneta, Lindsay Kosack, Marie-Louise Bergman, Nadia Duarte, Paula Matoso, Carlos P. Gonçalves, and Jocelyne Demengeot established and executed the ELISAs. All authors were enrolled in data analysis. Rute Castro, Júlia Costa, Lígia S. Nobre, Sónia Mendes, Ricardo A. Gomes, Micael C. Freitas, Marcos F. Q. Sousa, Jocelyne Demengeot, and Paula M. Alves wrote the manuscript. All authors approved the manuscript.

ORCID

Rute Castro  <https://orcid.org/0000-0002-0899-0649>

Lígia S. Nobre  <https://orcid.org/0000-0002-3060-2593>

Rute P. Eleutério  <https://orcid.org/0000-0002-1048-4411>

Mónica Thomaz  <https://orcid.org/0000-0002-3133-0278>

António Pires  <https://orcid.org/0000-0002-7713-6542>

Sandra M. Monteiro  <https://orcid.org/0000-0002-0345-8127>

Sónia Mendes  <https://orcid.org/0000-0003-0568-204X>

Ricardo A. Gomes  <http://orcid.org/0000-0001-7155-0059>

João J. Clemente  <https://orcid.org/0000-0002-3271-4994>

Marcos F. Q. Sousa  <https://orcid.org/0000-0003-3766-3900>

Filipe Pinto  <https://orcid.org/0000-0002-3838-0948>

Ana C. Silva  <http://orcid.org/0000-0003-3394-2793>

Micael C. Freitas  <https://orcid.org/0000-0001-7468-3471>

Ana R. Lemos  <https://orcid.org/0000-0002-3987-4771>

Onome Akpogheneta  <https://orcid.org/0000-0002-5213-4903>

Lindsay Kosack  <https://orcid.org/0000-0001-7266-0006>

Marie-Louise Bergman  <https://orcid.org/0000-0003-0691-4308>

Nadia Duarte  <https://orcid.org/0000-0002-4477-4492>
 Paula Matoso  <https://orcid.org/0000-0002-2315-7460>
 Júlia Costa  <https://orcid.org/0000-0001-7782-6319>
 Tiago M. Bandejas  <https://orcid.org/0000-0001-6089-6089>
 Patricia Gomes-Alves  <http://orcid.org/0000-0001-7245-6785>
 Carlos P. Gonçalves  <https://orcid.org/0000-0001-7225-1907>
 Jocelyne Demengeot  <https://orcid.org/0000-0002-4761-614X>
 Paula M. Alves  <http://orcid.org/0000-0003-1445-3556>

REFERENCES

- Amanat, F., Stadlbauer, D., Strohmaier, S., Nguyen, T. H. O., Chromikova, V., McMahon, M., Jiang, K., Arunkumar, G. A., Jurczyszak, D., Polanco, J., Bermudez-Gonzalez, M., Kleiner, G., Aydllo, T., Miorin, L., Fierer, D. S., Lugo, L. A., Kojic, E. M., Stoeber, J., Liu, S. T. H., ... Krammer, F. (2020). A serological assay to detect SARS-CoV-2 seroconversion in humans. *Nature Medicine (New York, NY, United States)*, 26, 1033–1036.
- André, M., Morelle, W., Planchon, S., Milhiet, P. E., Rubinstein, E., Mollicone, R., Chamot-Rooke, J., & Le Naour, F. (2007). Glycosylation status of the membrane protein CD9P-1. *Proteomics*, 7, 3880–3895. <https://doi.org/10.1002/pmic.200700355>
- Arbeitman, C. R., Auge, G., Blaustein, M., Bredeston, L., Corapi, E. S., Craig, P. O., Cossio, L. A., Dain, L., Alessio, C. D., Elias, F., Fernández, N. B., Gandola, Y. B., Gasulla, J., Gorojovsky, N., Gudesblat, G. E., Herrera, M. G., Ibañez, L. I., Idrovo, T., Rando, M. I., ... Zelada, A. M. (2020). Structural and functional comparison of SARS-CoV-2-spike receptor binding domain produced in *Pichia pastoris* and mammalian cells. *Scientific Reports*, 10, 21779. <https://doi.org/10.1038/s41598-020-78711-6>
- Baldi, L., Hacker, D. L., Meerschman, C., Wurm, F. M. (2012). Large-scale transfection of mammalian cells. In: Hartley J. (ed.), *Protein Expression in Mammalian Cells*. Methods in Molecular Biology (Methods and Protocols), vol 801. Humana Press. https://doi.org/10.1007/978-1-61779-352-3_2
- Ceroni, A., Maass, K., Geyer, H., Geyer, R., Dell, A., & Haslam, S. M. (2008). GlycoWorkbench: A tool for the computer-assisted annotation of mass spectra of glycans. *Journal of Proteome Research*, 7, 1650–1659. <https://doi.org/10.1021/pr7008252>
- Chin, C. L., Goh, J. B., Srinivasan, H., Liu, K. I., Gowher, A., Shanmugam, R., Lim, H. L., Choo, M., Tang, W. Q., Tan, A. H. M., Nguyen-Khuong, T., Tan, M. H., & Ng, S. K. (2019). A human expression system based on HEK293 for the stable production of recombinant erythropoietin. *Scientific Reports*, 9, 16768. <https://doi.org/10.1038/s41598-019-53391-z>
- Costa, J., Gatermann, M., Nimtz, M., Kandzia, S., Glatzel, M., & Conradt, H. S. (2018). N-Glycosylation of extracellular vesicles from HEK-293 and glioma cell lines. *Analytical Chemistry*, 90, 7871–7879. <https://doi.org/10.1021/acs.analchem.7b05455>
- Cummings, R. D., Darvill, A. G., Etzler, M. E., Hahn, M. G. (2017). Antibodies and lectins in glycan analysis. In A. Varki, R. D. Cummings, J. D. Esko, P. Stanley, G. W. Hart, M. Aebi, A. G. Darvill, T. Kinoshita, N. H. Packer, J. H. Prestegard, R. L. Schnaar, P. H. Seeberger (eds.), *Essentials of Glycobiology*, 3rd ed. 90, Cold Spring Harbor Laboratory Press.
- Durocher, Y., Perret, S., & Kamen, A. (2002). High-level and high-throughput recombinant protein production by transient transfection of suspension-growing human 293-EBNA1 cells. *Nucleic Acids Research*, 30, E9.
- Escrevente, C., Keller, S., Altevogt, P., & Costa, J. (2011). Interaction and uptake of exosomes by ovarian cancer cells. *BMC Cancer*, 11, 108. <https://doi.org/10.1186/1471-2407-11-108>
- Esposito, D., Mehalko, J., Drew, M., Snead, K., Wall, V., Taylor, T., Frank, P., Denson, J. P., Hong, M., Gulten, G., Sadtler, K., Messing, S., & Gillette, W. (2020). Optimizing high-yield production of SARS-CoV-2 soluble spike trimers for serology assays. *Protein Expression and Purification*, 174, 105686. <https://doi.org/10.1016/j.pep.2020.105686>
- Estes, B., Hsu, Y. R., Tam, L. T., Sheng, J., Stevens, J., & Haldankar, R. (2015). Uncovering methods for the prevention of protein aggregation and improvement of product quality in a transient expression system. *Biotechnology Progress*, 31, 258–267. <https://doi.org/10.1002/btpr.2021>
- González-Feliciano, J. A., Akamine, P., Capó-Vélez, C. M., Delgado-Vélez, M., Dussupt, V., Krebs, S. J., Wojna, V., Polonis, V. R., Baerga-Ortiz, A., & Lasalde-Dominicci, J. A. (2020). A recombinant gp145 Env glycoprotein from HIV-1 expressed in two different cell lines: Effects on glycosylation and antigenicity. *PLoS One*, 15, e0231679. <https://doi.org/10.1371/journal.pone.0231679>
- Grant, O. C., Montgomery, D., Ito, K., & Woods, R. J. (2020). Analysis of the SARS-CoV-2 spike protein glycan shield reveals implications for immune recognition. *Scientific Reports*, 10, 14991. <https://doi.org/10.1038/s41598-020-71748-7>
- Henderson, R., Edwards, R. J., Mansouri, K., Janowska, K., Stalls, V., Kopp, M., Haynes, B. F., & Acharya, P. (2020). Glycans on the SARS-CoV-2 spike control the receptor binding domain conformation. *bioRxiv*. <https://doi.org/10.1101/2020.06.26.173765>
- Herrera, N. G., Morano, N. C., Celikgil, A., Georgiev, G. I., Malonis, R. J., Lee, J. H., Tong, K., Vergnolle, O., Massimi, A. B., Yen, L. Y., Noble, A. J., Kopylov, M., Bonanno, J. B., Garrett-Thomson, S. C., Hayes, D. B., Bortz, R. H., Wirchniaski, A. S., Florez, C., Laudermilch, E., ... Almo, S. C. (2021). Characterization of the SARS-CoV-2 S protein: Biophysical, biochemical, structural, and antigenic analysis. *ACS Omega*, 6(1), 85–102. <https://doi.org/10.1021/acsomega.0c03512>
- Jäger, V., Groenewold, J., Krüger, D., Schwarz, D., Vollmer, V. (2015). High-titer expression of recombinant antibodies by transiently transfected HEK 293-6E cell cultures. *BMC Proc*, 9, P40. <https://doi.org/10.1186/1753-6561-9-S9-P40>
- Johari, Y. B., Jaffé, S. R., Scarrott, J. M., Johnson, A. O., Mozzanino, T., Pohle, T. H., Maisuria, S., Bhayat-Cammack, A., Lambiase, G., Brown, A. J., Lan Tee, K., Jackson, P. J., Seng Wong, T., Dickman, M. J., Sargur, R., & James, D. C. (2020). Production of trimeric SARS-CoV-2 spike protein by CHO cells for serological COVID-19 testing. *Biotechnology and Bioengineering*, 118, 1–9. <https://doi.org/10.1002/bit.27615>
- Li, T., Zheng, Q., Yu, H., Wu, D., Xue, W., Zhang, Y., Huang, X., Zhou, L., Zhang, Z., Zha, Z., Chen, T., Wang, Z., Chen, J., Sun, H., Deng, T., Wang, Y., Chen, Y., Zhao, Q., Zhang, J., ... Xia, N. (2020). Characterization of the SARS-CoV-2 spike in an early prefusion conformation. *bioRxiv*. <https://doi.org/10.1101/2020.03.16.994152>
- Lin, C. Y., Huang, Z., Wen, W., Wu, A., Wang, C., & Niu, L. (2015). Enhancing protein expression in HEK-293 cells by lowering culture temperature. *PLoS One*, 10, e0123562. <https://doi.org/10.1371/journal.pone.0123562>
- Machado, E., Kandzia, S., Carilho, R., Altevogt, P., Conradt, H. S., & Costa, J. (2011). N-Glycosylation of total cellular glycoproteins from the human ovarian carcinoma SKOV3 cell line and of recombinantly expressed human erythropoietin. *Glycobiology*, 21, 376–386. <https://doi.org/10.1093/glycob/cwq170>
- Mason, M., Sweeney, B., Cain, K., Stephens, P., & Sharfstein, S. (2014). Reduced culture temperature differentially affects expression and biophysical properties of monoclonal antibody variants. *Antibodies*, 3, 253–271.
- Nettleship, J. E., Assenberg, R., Diprose, J. M., Rahman-Huq, N., & Owens, R. J. (2010). Recent advances in the production of proteins in insect and mammalian cells for structural biology. *Journal of Structural Biology*, 172, 55–65. <https://doi.org/10.1016/j.jsb.2010.02.006>
- Okba, N. M. A., Müller, M. A., Li, W., Wang, C., GeurtsvanKessel, C. H., Corman, V. M., Lamers, M. M., Sikkema, R. S., Bruin, E., de, Chandler, F. D., Yazdanpanah, Y., Hingrat, Q.L.e, Descamps, D., Houhou-Fidouh, N., Reusken, C. B. E. M., Bosch, B.-J., Drosten, C., Koopmans, M. P. G., & Haagmans, B. L. (2020). Severe acute respiratory syndrome coronavirus 2-specific antibody responses in coronavirus disease patients. *Emerging Infectious Diseases*, 26(7), 1478–1488. <https://doi.org/10.3201/eid2607.200841>

- Perera, R. A. P. M., Mok, C. K. P., Tsang, O. T. Y., Lv, H., Ko, R. L. W., Wu, N. C., Yuan, M., Leung, W. S., Chan, J. M. C., Chik, T. S. H., Choi, C. Y. C., Leung, K., Chan, K. H., Chan, K. C. K., Li, K. C., Wu, J. T., Wilson, I. A., Monto, A. S., Poon, L. L. M., & Peiris, M. (2020). Serological assays for severe acute respiratory syndrome coronavirus 2 (SARS-CoV-2), March 2020. *Eurosurveillance*, 25(16), 2000421. <https://doi.org/10.2807/1560-7917.ES.2020.25.16.2000421>
- Pham, P. L., Kamen, A., & Durocher, Y. (2006). Large-scale transfection of mammalian cells for the fast production of recombinant protein. *Molecular Biotechnology*, 34(2), 225–237. <https://doi.org/10.1385/MB:34:2:225>
- Pham, P. L., Perret, S., Cass, B., Carpentier, E., St-Laurent, G., Bisson, L., Kamen, A., & Durocher, Y. (2005). Transient gene expression in HEK293 cells: Peptone addition posttransfection improves recombinant protein synthesis. *Biotechnology and Bioengineering*, 90, 332–344. <https://doi.org/10.1002/bit.20428>
- Shajahan, A., Supekar, N. T., Gleinich, A. S., & Azadi, P. (2020). Deducing the N- and O-glycosylation profile of the spike protein of novel coronavirus SARS-CoV-2. *Glycobiology*, 30(12), 981–988. <https://doi.org/10.1093/glycob/cwaa042>
- Simone, M. S., Randolph, J. K., Gabriele, G., Martina, K., Friedrich, D., & Friedrich, S. (2003). Higher expression of Fab antibody fragments in a CHO cell line at reduced temperature. *Biotechnology and Bioengineering*, 84, 433–438. <https://doi.org/10.1002/bit.10793>
- Stadlbauer, D., Amanat, F., Chromikova, V., Jiang, K., Strohmeier, S., Arunkumar, G. A., Tan, J., Bhavsar, D., Capuano, C., Kirkpatrick, E., Meade, P., Brito, R. N., Teo, C., McMahon, M., Simon, V., & Krammer, F. (2020). SARS-CoV-2 seroconversion in humans: A detailed protocol for a serological assay, antigen production, and test setup. *Current Protocols in Microbiology*, 57, e100. <https://doi.org/10.1002/cpmc.100>
- Stuible, M., Gervais, C., Lord-Dufour, S., Perret, S., Abbe, D. L., Schrag, J., St-Laurent, G., & Durocher, Y. (2020). Rapid, high-yield production of full-length SARS-CoV-2 spike ectodomain by transient gene expression in CHO cells. *Journal of Biotechnology*, 326, 21–27. <https://doi.org/10.1016/j.jbiotec.2020.12.005>
- Walls, A. C., Park, Y. J., Tortorici, M. A., Wall, A., McGuire, A. T., & Veesler, D. (2020). Structure, function, and antigenicity of the SARS-CoV-2 spike glycoprotein. *Cell*, 181(2), 281–292. <https://doi.org/10.1016/j.cell.2020.02.058>
- Wang, Q., Zhang, Y., Wu, L., Niu, S., Song, C., Zhang, Z., Lu, G., Qiao, C., Hu, Y., Yuen, K. Y., Wang, Q., Zhou, H., Yan, J., & Qi, J. (2020). Structural and functional basis of SARS-CoV-2 entry by using human ACE2. *Cell*, 181, 894–904.
- Watanabe, Y., Allen, J. D., Wrapp, D., McLellan, J. S., & Crispin, M. (2020). Site-specific glycan analysis of the SARS-CoV-2 spike. *Science*, 369, 330–333. <https://doi.org/10.1126/science.abb9983>
- Weiss, S., Klingler, J., Hioe, C., Amanat, F., Baine, I., Arinsburg, S., Kojic, E. M., Stoeber, J., Liu, S., Jurczynszak, D., Bermudez-Gonzalez, M., Simon, V., Krammer, F., & Zolla-Pazner, S. (2020). A high through-put assay for circulating antibodies directed against the S protein of severe acute respiratory syndrome coronavirus 2. *Journal of Infectious Diseases*, 222(10), 1629–1634. <https://doi.org/10.1093/infdis/jiaa531>
- Wrapp, D., Wang, N., Corbett, K. S., Goldsmith, J. A., Hsieh, C. L., Abiona, O., Graham, B. S., & McLellan, J. S. (2020). Cryo-EM structure of the 2019-nCoV spike in the prefusion conformation. *Science*, 367(6483), 1260–1263. <https://doi.org/10.1126/science.abb2507>
- Zhou, P., Yang, X. L., Wang, X. G., Hu, B., Zhang, L., Zhang, W., Si, H. R., Zhu, Y., Li, B., Huang, C. L., Chen, H. D., Chen, J., Luo, Y., Guo, H., Jiang, R. D., Liu, M. Q., Chen, Y., Shen, X. R., Wang, X., ... Shi, Z. L. (2020). A pneumonia outbreak associated with a new coronavirus of probable bat origin. *Nature*, 579, 270–273.

SUPPORTING INFORMATION

Additional Supporting Information may be found online in the supporting information tab for this article.

How to cite this article: Castro, R., Nobre, L. S., Eleutério, R. P., Thomaz, M., Pires, A., Monteiro, S. M., Mendes, S., Gomes, R. A., Clemente, J. J., Sousa, M. F. Q., Pinto, F., Silva, A. C., Freitas, M. C., Lemos, A. R., Akpogheneta, O., Kosack, L., Bergman, M.-L., Duarte, N., Matoso, P., ... Alves P. M. (2021). Production of high-quality SARS-CoV-2 antigens: Impact of bioprocess and storage on glycosylation, biophysical attributes, and ELISA serologic tests performance. *Biotechnology and Bioengineering*. 118, 2202–2219. <https://doi.org/10.1002/bit.27725>